Kobe University Repository : Kernel

PDF issue: 2025-12-05

Roles of Cdc42 and Rac in Bergmann glia during cerebellar corticogenesis

Sakamoto, Isao ; Ueyama, Takehiko ; Hayashibe, Masakazu ; Nakamura, Takashi ; Mohri, Hiroaki ; Kiyonari, Hiroshi ; Shigyo, Michiko ; Tohda…

(Citation)
Experimental Neurology,302:57-67

(Issue Date)
2018-04

(Resource Type)
journal article

(Version)
Accepted Manuscript

(Rights)
© 2018 Elsevier B.V.
This manuscript version is made available under the CC-BY-NC-ND 4.0 license
http://creativecommons.org/licenses/by-nc-nd/4.0/

(URL)
https://hdl.handle.net/20.500.14094/90006402

KOBE UNIVERSITY

Roles of Cdc42 and Rac in Bergmann glia during cerebellar corticogenesis

Isao Sakamoto[1,†], Takehiko Ueyama[1,†,*], Masakazu Hayashibe[1], Takashi Nakamura[1], Hiroaki Mohri[1], Hiroshi Kiyonari[2], Michiko Shigyo[3], Chihiro Tohda[3], Naoaki Saito[1,*]

[1]Laboratory of Molecular Pharmacology, Biosignal Research Center, Kobe University, Kobe 657-8501, Japan; [2]Animal Resource Development Unit and Genetic Engineering Team, RIKEN Center for Life Science Technologies, Kobe 650-0047, Japan; [3]Division of Neuromedical Science, Department of Bioscience, Institute of Natural Medicine, University of Toyama, Toyama 930-0194, Japan

Keywords: astrocytes, cerebellar development, cerebellar granule neurons, gliophilic migration, neuregulin 1, Notch3, radial migration, Rho-family small GTPases

Running title: Cdc42 and Rac in BG in cerebellar lamination

† These authors contributed equally to this work.

* Corresponding author: Takehiko UEYAMA and Naoaki SAITO
1-1 Rokkodai-cho, Nada-ku, Kobe 657-8501, Japan,
Tel: +81-78-803-5962, Fax: +81-78-803-5971
E-mails: tueyama@kobe-u.ac.jp and naosaito@kobe-u.ac.jp

ABSTRACT

Bergmann glia (BG) are important in the inward type of radial migration of cerebellar granule neurons (CGNs). However, details regarding the functions of Cdc42 and Rac in BG for radial migration of CGN are unknown. To examine the roles of Cdc42 and Rac in BG during cerebellar corticogenesis, mice with a single deletion of Cdc42 or Rac1 and those with double deletions of Cdc42 and Rac1 under control of the glial fibrillary acidic protein (GFAP) promoter: *GFAP-Cre;Cdc42*$^{flox/flox}$ (Cdc42-KO), *GFAP–Cre;Rac1*$^{flox/flox}$ (Rac1-KO), and *GFAP-Cre;Cdc42* $^{flox/flox}$*;Rac1*$^{flox/flox}$ (Cdc42/Rac1-DKO) mice, were generated. Both Cdc42-KO and Rac1-KO mice, but more obviously Cdc42-KO mice, had disturbed alignment of BG in the Purkinje cell layer (PCL). We found that Cdc42-KO, but not Rac1-KO, induced impaired radial migration of CGNs in the late phase of radial migration, leading to retention of CGNs in the inferior half of the molecular layer (ML). Cdc42-KO, but not Rac1-KO, mice also showed aberrantly aligned Purkinje cells (PCs). These phenotypes were exacerbated in Cdc42/Rac1-DKO mice. Alignment of BG radial fibers in the ML and BG endfeet at the pial surface of the cerebellum evaluated by GFAP staining was disturbed and weak in Cdc42/Rac1-DKO mice, respectively. Our data indicate that that Cdc42 and Rac, but predominantly Cdc42, in BG play important roles during the late phase of radial migration of CGNs. We also report here that Cdc42 is involved in gliophilic migration of CGNs, in contrast to Rac, which is more closely connected to regulating neurophilic migration.

HIGHLIGHTS:

- Cdc42-KO, Rac1-KO, Cdc42/Rac1-DKO mice under control of the GFAP promoter were made.
- Cdc42-KO and Rac1-KO mice had disturbed alignment of BG in the PCL.
- Cdc42-KO mice showed aberrantly aligned PCs.
- Cdc42-KO mice showed impaired radial migration of CGNs in the late phase.
- The phenotypes observed in Cdc42-KO mice were exacerbated in Cdc42/Rac1-DKO mice.

INTRODUCTION

Astrocytes play important roles in the establishment and maintenance of numerous brain functions, including control of the blood-brain barrier; regulation of blood flow; supply of energy metabolites to neurons; synaptic function; extracellular balance of ions, fluids, and transmitters (Pekny et al., 2016). Astrocytes also play pivotal roles in corticogenesis/lamination of the cerebrum (Borrell and Gotz, 2014) and cerebellum during development (Buffo and Rossi, 2013), when they exist as radial glia (RG) and Bergmann glia (BG). RG function as progenitor cells giving rise to both neurons and glial cells, but also exert scaffolding activity for migrating neurons during corticogenesis (Borrell and Gotz, 2014). BG derive directly from morphological transformation of RG and are unique astrocytes in the cerebellum that play essential roles in cerebellar corticogenesis (Buffo and Rossi, 2013).

The cerebellar cortex consists of three layers: the molecular layer (ML), the Purkinje cell layer (PCL), and the internal granule layer (IGL) (Chedotal, 2010). BG are located at the PCL and extend their radial processes (also referred to as BG fibers or BG radial fibers) across the ML. These processes terminate at the pial surface of the cerebellum in endfeet (Yamada and Watanabe, 2002), and are involved in the development of the IGL and the maturation of Purkinje cells (PCs) (Buffo and Rossi, 2013; Xu et al., 2013). Cerebellar granule neurons (CGNs) proliferating and differentiating in the EGL begin to inwardly and radially migrate to form the IGL. This is a characteristic phenomenon of cerebellar corticogenesis (Chedotal, 2010). This inward type of radial migration begins at birth and is completed by P20 in mice (Hatten et al., 1997). This process peaks between P7 and P12 (Komuro et al., 2001). In contrast, PCs originate at the ventricular zone at E12, outwardly migrate to the PCL from E13 to E17, and establish monolayer alignment by P7 (Yamada and Watanabe, 2002; Yuasa et al., 1991). BG are reported to be involved in the inward type of radial migration (Rakic, 1971). However, the detailed functional mechanisms of BG during radial migration of CGNs are still unclear.

Cdc42 and Rac (Rac1, Rac2, and Rac3) are the best characterized members of the Rho family of small guanosine triphosphatases (GTPases), which play fundamental roles in a wide

variety of cellular processes, including establishment/maintenance of actin-based cytoskeleton and neuronal polarity (Bosco et al., 2009; Takano et al., 2015). We recently described the functions of Rac in CGNs during cerebellar corticogenesis using CGN-specific Rac1/Rac3 double-knockout (DKO) mice, which show severely impaired radial migration of CGNs during the early phase and have defects in the IGL (Nakamura et al., 2017). However, the roles and functions of Cdc42 and Rac in BG during cerebellar corticogenesis remain unknown.

To examine the roles of Cdc42 and Rac in BG during cerebellar corticogenesis (radial migration of CGNs during cerebellar development), we generated mice with deletions of Cdc42, Rac1, or Cdc42 and Rac1 under control of the glial fibrillary acidic protein (GFAP) promoter: *GFAP–Cre;Cdc42*$^{flox/flox}$ (Cdc42-KO), *GFAP–Cre;Rac1*$^{flox/flox}$ (Rac1-KO), and *GFAP–Cre;Cdc42*$^{flox/flox}$*;Rac1*$^{flox/flox}$ (Cdc42/Rac1-DKO). Here, we report that Cdc42-KO, but not Rac1-KO, mice have impaired radial migration of CGNs during the late phase of the radial migration of CGNs, which leads to the retention of CGNs in the inferior half of the ML.

MATERIALS AND METHODS

Animals

All animal experiments were conducted in accordance with the guidelines of Kobe University and RIKEN. The *Cdc42*^{flox} (Ueyama et al., 2014) and *GFAP-Cre;Rac1*^{flox} (hereafter referred to as Rac1-KO) mice (Ishii et al., 2016) have been described previously. The *GFAP-Cre;Cdc42*$^{flox/+}$ progeny of *Cdc42*$^{flox/flox}$ and *GFAP-Cre* mice (Bajenaru et al., 2002) were back-crossed with *Cdc42*$^{flox/flox}$ mice to obtain *GFAP-Cre;Cdc42*$^{flox/flox}$ (hereafter referred to as Cdc42-KO) mice. These mice were in turn backcrossed to *Cdc42*$^{flox/flox}$ mice to generate experimental animals. *GFAP-Cre;Rac1*$^{flox/flox}$ (Rac1-KO) mice were backcrossed with *Rac1*$^{flox/flox}$ mice to generate experimental animals. The *GFAP-Cre;Cdc42*$^{flox/+}$*;Rac1*$^{flox/+}$ progeny of *GFAP-Cre;Cdc42*$^{flox/flox}$ and *Rac1*$^{flox/flox}$ mice were back-crossed with *Cdc42*$^{flox/flox}$*;Rac1*$^{flox/flox}$ mice to obtain *GFAP-Cre;Cdc42*$^{flox/flox}$*;Rac1* $^{flox/flox}$ (hereafter referred to as Cdc42/Rac1-DKO) mice. These mice were in turn backcrossed with *Cdc42*$^{flox/flox}$*;Rac1*$^{flox/flox}$ mice to generate experimental animals. *CAG-STOP*^{flox}*-tdTomato* (Ai9) reporter mice were purchased from the Jackson Laboratory and backcrossed with *GFAP-Cre* mice to generate *GFAP-Cre;tdTomato* mice, which were then used to examine the effect of the GFAP promoter. The offspring of these mice were genotyped by polymerase chain reaction (PCR) using the following primers: 5'-ACTCCTTCATAAAGCCCTCG-3' (forward) and 5'-ATCACTCGTTGCATCGACCG-3' (reverse) for *GFAP-Cre,* 5'-ATCGGTCACTGTTCTACTTTG-3' and 5'-TACTGCTATGACTGAAAACCTC-3' for Cdc42^{flox}, 5'-ATTTTCTAGATTCCACTTGTGAAC-3' and 5'-ATCCCTACTTCCTTCCAACTC-3' for *Rac1*^{flox}, and 5′-GGCATTAAAGCAGCGTATCC-3′ and 5′-CTGTTCCTGTACGGCATGG-3′ for *tdTomato*. Wild type (WT) C57BL/6 mice were purchased from Clea Japan.

Antibodies

The following specific antibodies (Abs) were used (monoclonal unless indicated): anti-Cdc42 (44/CDC42, BD Biosciences, 1/500); anti-Rac1 (23A8, Millipore, 1/500); polyclonal anti-GFAP (Z0334, DAKO, 1/1000); anti-Cre recombinase (2D8, Millipore, 1/1000); polyclonal anti-calbindin (AB1778, Millipore, 1/2,000); polyclonal anti-PKCγ (sc-211, Santa Cruz Biosciences, 1/3000); anti-NeuN (A60, Millipore, 1/100); polyclonal anti-BLBP (BLBP-Rb-Af400-1, Frontier Institute Co., Ltd., Japan, 1/200); polyclonal

anti-active caspase-3 (G7481, Promega, 1/250), anti-EGFR (D38B1, CST, 1/1000), anti-ErbB2 (D8F12, CST, 1/500), anti-FGFR1 (D8E4, CST, 1/1000), anti-FGFR3 (EPR2304(3), Abcam, 1/1000), polyclonal anti-neuregulin 1 type III (ab23248, Abcam, 1/200), polyclonal anti-Notch3 (ab23426, Abcam, 1/200), and anti-glutamine synthetase (GS, GS-6, Millipore, 1/100). Alexa488- and Alexa564-conjugated secondary Abs were obtained from Invitrogen. Horseradish peroxidase (HRP)-conjugated anti-tubulin-α Abs were obtained from MBL International (Japan).

Cell culturing and RNA interference

Primary astrocyte cultures were prepared from mouse cerebral cortex at postnatal day 1 or 2 (P1–2), as previously described (Ishii et al., 2016). Briefly, dissected cerebral cortices were dissociated using a neuron dissociation solution (Wako Pure Chemical Industries, Japan), and cultured in Eagle's Minimum Essential Medium (Wako) supplemented with 10% fetal bovine serum (FBS; Nichirei Biosciences, Japan) and penicillin-streptomycin (PS) solution (Wako) in 25-cm^2 flasks (2 brains per flask) (Corning Inc.). After 5–7 days, the flasks were subjected to 1 hour of continuous shaking to obtain purified astrocytes. Cell lysates were used for immunoblotting experiments and DNA microarray analysis.

U-87 MG astrocytic cells (ATCC) were maintained in DMEM (Wako) containing 10% FBS and PS. The validated RNAi sequences for *RAC1* (siRAC1-618: 5′-CCTTTGTACGCTTTGCTCA-3′ (Ishii et al., 2016; Ueyama et al., 2006)) and *CDC42* (siCDC42-197: 5′-GATTACGACCGCTGAGTTA-3′ (Qin et al., 2010; Ueyama et al., 2014)) have been previously described. The siRNAs for *RAC1*, *CDC42*, and a control siRNA (MISSION Universal Negative Control) were purchased from Sigma-Aldrich. The siRNAs were transfected into U87 cells using RNAiMAX (Invitrogen), and the cells were used for experiments 48 h after transfection.

MDCK cells with stable expression of the short hairpin RNA (shRNA) expression plasmid (*pSUPER*, OrigoEngine; $MDCK^{cont}$) or the shRNA expression plasmid containing a *Cdc42*-targeting sequence ($MDCK^{Cdc42\text{-}KD}$) were established as described previously (Ueyama et al., 2014), and maintained in DMEM containing 10% FBS, PS, and 3 mg/ml G418 solution (Wako).

All cells were maintained in a 5% CO_2 humidified incubator at 37°C.

Reverse transcriptase PCR

Reverse transcriptase PCR (RT-PCR) was performed using 1 μg of total RNA obtained from the primary astrocytes of WT mice using SuperScript III reverse transcriptase (Invitrogen) and random primers. The following primer pairs were used for PCR (30 cycles): 5′-GCAGACAGACGTGTTCTTAATTTGC-3′ and 5′-TGTAACAAAAACTTGGCATCAAATGCG-3′ for *Rac1* (454 bp), 5′-CCCACACACACCCATCCTTC-3′ and 5′-TGGAGCTATATCCCAGAAAAAGGAG-3′ for *Rac3* (440 bp), and 5′-GAAATGCAGACAATTAAGTGTGTTGTTG-3′ and 5′-TCATAGCAGCACACACCTGCGGCT-3′ for *Cdc42* (579 bp).

Immunoblotting

Cells were lysed in homogenizing buffer (Ueyama et al., 2007) by sonication in the presence of a protease inhibitor cocktail, a protein phosphatase inhibitor cocktail (Nacalai Tesque, Japan), and 1% Triton X-100. Total lysates were centrifuged at 800 × *g* for 5 minutes at 4°C, and the supernatants were subjected to sodium dodecyl sulfate polyacrylamide gel electrophoresis, followed by immunoblotting for 16 hours at 4°C using primary Abs diluted in phosphate buffered saline (PBS) containing 0.03% Triton X-100 (PBS-0.03T). The bound primary Abs were detected using secondary Ab-HRP conjugates using the ECL detection system (Bio-Rad Labolatories).

Section preparation, immunohistochemistry, and X-gal and Nissl stainings

Animals were deeply anesthetized using pentobarbital, and transcardially perfused with ice-cold 0.9% saline solution, and subsequently with 4% paraformaldehyde (PFA) in 0.1 M phosphate buffer (PB) (pH 7.4) (Ueyama et al., 2016). Brains were dissected and post-fixed overnight in the same fresh fixative.

Twenty-μm-thick sagittal sections of the cerebrum and cerebellum were obtained. After permeabilization with PBS-0.3T, the cerebellar sections were incubated overnight with primary Abs (GFAP and Cre, calbindin and Cre, BLBP and Cre, neuregulin 1 and GS, or Notch3 and GS) in PBS-0.03T at 4°C, followed by incubation with Alexa488- and Alexa568-conjugated secondary Abs for 1 hour at 23°C. To obtain two-dimensional (2D) reconstructed images, 60-μm-thick cerebellar sections were incubated in 0.2 mg/mL trypsin (T1426, Sigma-Aldrich) for 30 minutes at 23°C, and then immunostained using GFAP and

Cre primary Abs and Alexa488- and Alexa568-conjugated secondary Abs. The resulting labeling was observed using an LSM700 confocal laser microscope (Carl Zeiss).

To perform diaminobenzidine (DAB) immunohistochemistry, the cerebellar sections were incubated overnight with an anti-NeuN, anti-Cre, anti-PKCγ, anti-GFAP, active caspase-3, anti-neuregulin 1, or anti-Notch3 Abs in PBS-0.03T at 4°C, followed by DAB staining using a Vectastain ABC kit (Vector Laboratories). In the case of active caspase-3 staining, sections were counterstained with methyl green (Muto Pure Chemicals, Japan). X-gal staining (to detect β-galactosidase expression), X-gal staining with GFAP immunostaining, and Nissl staining have previously been described (Ueyama et al., 2014). The slides were photographed using a light microscope (Axioplan II; Carl Zeiss) and a DP26 camera (Olympus).

Rac1 activation (pull down) assay

The Rac1 activation assay was performed using a Rac1 activation assay kit (Cell Biolabs) as described previously (Ueyama et al., 2006). Briefly, $MDCK^{cont}$ and $MDCK^{Cdc42\text{-}KD}$ cells grown in 10-cm dishes with DMEM containing 10% FBS were harvested using 300 μl of lysis/wash buffer. Cell lysates were centrifuged for 5 min at 3,000 x g and the resulting supernatants were measured with a bicinchoninic acid (BCA) protein assay kit (Thermo Fisher Scientific). The same amount of each supernatant was mixed with GST-CRIB(PAK1) conjugated to agarose beads and rocked at 4°C for 1 h. For positive control experiments, GTPγS was added to the resulting supernatants described above (final concentration 100μM). After rocking for 15min at RT, the supernatants were mixed with CRIB(PAK1)-conjugated agarose beads and again rocked at 4°C for 1h. After three washes, the beads were resuspended in Laemmli sample buffer, and the proteins bound to CRIB(PAK1) were separated by SDS-PAGE and probed with a Rac1 antibody.

EdU pulse-labeling

EdU detection was performed using a Click-iT EdU AlexaFluor488 Imaging kit (Invitrogen) and a confocal laser microscope as described previously (Nakamura et al., 2017). Briefly, P3.5 mice (control and Cdc42/Rac1-DKO) were intraperitoneally injected with 15 mg/kg 5-ethynyl-2'-deoxyuridine (EdU) dissolved in PBS. Cerebella were fixed 24 h after injection, and sagittal sections were used for the analysis of proliferation of cells around the PCL.

DNA microarray

Total RNA from WT primary astrocytes and U87 cells (transfected with 0.75 nM control siRNA or 0.25 nM siCDC42-197 + 0.5 nM siRAC1-618) was extracted using NucleoSpin RNA (MACHEREY-NAGEL GmbH & Co. KG). The quality and quantity of RNA were determined using an Agilent 2100 BioAnalyzer, and gene expression profiles were examined using the SurePrint G3 Mouse GE 8×60K Microarray and the SurePrint G3 Human GE v3 8×60K Microarray kits (Agilent Technologies). The background-subtracted signal intensity was subjected to 75th percentile normalization for inter-array comparison. The value was used as normalized signal intensity, and the ratio (Log2 ratio) of the normalized value of each gene (CDC42/RAC1-DKD/control) is presented.

Statistics

The number of cells positive for Nissl, NeuN, Cre, or PKCγ in a 350-μm-wide section was counted; the number of active caspase-3-positive cells per cerebellum was quantified. All data are presented as the mean ± SEM. Two groups were compared using unpaired Student's *t*-tests. For comparisons of more than two groups, one-way analysis of variance (ANOVA) and Bonferroni's *post hoc* test of pairwise group differences were used. Statistical analyses were performed using Prism 6.0 software (GraphPad).

Data availability

DNA microarray data are available in the NCBI Gene Expression Omnibus (GEO, www.ebi.ac.uk/arrayexpress) under accession number GSE106143, which consists of GSE106141 (primary astrocytes) and GSE106142 (U87 astrocytic cells).

RESULTS

Generation of Rac1-KO, Cdc42-KO, and Cdc42/Rac1-DKO mice in astrocytes

We have previously reported that of the three members of *Rac* family, only *Rac1* is expressed in primary astrocytes (Ishii et al., 2016). Here we detected *Cdc42* mRNA in primary astrocytes using RT-PCR. We also detected mRNA for *Rac1*, which is one of two epithelial subtypes of *Rac* (*Rac1* and *Rac3*) (Heasman and Ridley, 2008), but not *Rac3* (Fig. 1A). Based on this result, we generated mice with *Rac1-KO*, *Cdc42*-KO, and *Cdc42/Rac1*-DKO in astrocytes using a *GFAP-Cre* transgenic (TG) mouse (Fig. 1B). The patterns of *GAFP-Cre*-driven recombination in the cerebrum and cerebellum were assessed using X-gal staining. X-gal staining was positive in GFAP-positive astrocytes in the cerebrum and cerebellum of *GFAP-Cre* mice, but not in the control (*GFAP-Cre*$^{-/-}$) mice (Fig. 1C). The linearly aligned X-gal-positive cells in the PCL of the cerebellum were confirmed to be BG, and not PCs, through immunostaining for calbindin, which is a maker for PCs (Hatten et al., 1997), and GFAP, which is a marker for BG (Yamada and Watanabe, 2002) (Fig. 1D). KO of *Rac1* and *Cdc42* in astrocytes was confirmed by immunoblotting using primary astrocytes obtained from Rac1-KO and Cdc42-KO mice (Fig. 1E).

Abnormalities in the cerebellar cortex, but not cerebral cortex, in Cdc42-KO mice

Rac1-KO, Cdc42-KO, and Cdc42/Rac1-DKO mice had no apparent behavioral abnormalities. We histologically examined the cerebral cortex and the cerebellar cortex in these three KO mice lines using Nissl staining. Although no apparent abnormalities were observed in the layering of the cerebral cortex in these KO mice lines (Fig. 2A), the cerebellar cortex was abnormal in Cdc42-KO mice. There were densely stained small cells in the lower half of the ML, and disturbed alignment of the lightly stained PCs in the PCL of Cdc42-KO mice (Fig. 2B). These abnormalities were not observed in Rac1-KO mice, but were markedly exacerbated in Cdc42/Rac1-DKO mice, as demonstrated by the number of small cells in the ML (Fig. 2B). These phenotypes were detected throughout the Cdc42-KO and Cdc42/Rac1-DKO cerebella (Fig. 2C); furthermore, the sizes of the cerebellum in the

Rac1/Cdc42-DKO mice were smaller than that in the controls (Fig. 2C).

To examine the reason why the additional Rac1-KO exacerbates the phenotypes of Cdc42-KO in the cerebellum, the amount of active Rac1 was assayed in $MDCK^{cont}$ and $MDCK^{Cdc42\text{-}KD}$ cells (Ueyama et al., 2014). Although total amounts of Rac1 were comparable between $MDCK^{cont}$ and $MDCK^{Cdc42\text{-}KD}$ cells (also refer to Fig. S2A), the amount of active Rac1 in $MDCK^{Cdc42\text{-}KD}$ cells was larger both in the resting condition (with 10% FBS) and after treatment with GTPγS than that in $MDCK^{cont}$ cells (Fig. S1).

Aberrant positioning of CGNs and BG in Cdc42-KO mice

To identify the densely stained small cells in the lower half of the ML, we performed immunostaining for NeuN, which is a maker of mature CGNs. We also stained for Cre recombinase (Cre), to identify KO cells; PKCγ, a marker of mature PCs; and GFAP, a marker of astrocytes. Small cells in the lower half of the ML in the Cdc42-KO and Cdc42/Rac1-DKO mice were positive for NeuN (Fig. 3A). Disturbed alignment of Cre-positive BG was observed in both the Rac1-KO and Cdc42-KO mice (Fig. 3B, 6A and 6B). Disturbed alignment of PKCγ-positive PCs was also observed in Cdc42-KO mice, but not in Rac1-KO mice (Fig. 3C). These aberrant localizations of CGNs and BG in the Cdc42-KO mice were markedly exacerbated in Cdc42/Rac1-DKO mice. The number of NeuN–, Cre–, or PKCγ–positive cells was counted and statistically analyzed; no statistical difference was observed among the control, Rac1-KO, Cdc42-KO, and Cdc42/Rac1-DKO mice (Fig. 3A, B, and C). In Cdc42/Rac1-DKO mice, the border of GFAP immunostaining between the ML and the IGL was obscure (Fig. 3D).

Impaired radial migration in Cdc42-KO and Cdc42/Rac1-KO mice during the development of cerebellar cortex

To examine the time at which the aberrant localization of CGNs in the lower half of the ML occurs in Cdc42-KO and Cdc42/Rac1-DKO mice, the development of the cerebellar cortex was monitored from postnatal day 3 (P3) to P21. During normal cerebellar

development, the EGL is observed by E16, after which the progenitor cells of the CGNs proliferate in the EGL. After proliferation, the CGN progenitors begin to differentiate in the deep layer of the EGL. Subsequently, the differentiated CGNs begin to inwardly and radially migrate up to P20 (Hatten et al., 1997).

Retention of small, densely stained CGNs in the lower parts of the ML was observed in Cdc42-KO and Cdc42/Rac1-DKO mice beginning at P5 (Fig. 4). At P10, retention of CGNs in the ML and aberrantly localized PCs became more apparent (Fig. 4). Retention of CGNs in the lower half of the ML was still observed in Cdc42-KO and Cdc42/Rac1-DKO mice at P21, at which point cerebellar development is complete in control (WT) mice (Fig. 4). These results suggest that impaired inward radial migration of CGNs during cerebellar development leads to retention of CGNs in the lower half of the ML.

To examine the effect of DKO of Cdc42 and Rac1 on the proliferation of BG, we applied EdU pulse-labeling to the cerebellum at P3.5, when BG, but not CGNs, migrate to and proliferate around the predicted PCL (Yamada and Watanabe, 2002). No significant difference in the number of EdU-labeled cells around the predicted PCL was observed between control and Cdc42/Rac1-DKO mice at 24 h after EdU injection (Fig. 5A). As expected, the number of EdU-labeled cells in the EGL was not significantly different between control and Cdc42/Rac1-DKO mice.

To further examine the effect of Cdc42 and Rac1 DKO on cell death, apoptotic cells were examined using immunostaining for active caspase-3 at P4. The number of active caspase-3 positive cells around the predicted PCL was much lower than that in the CGN-specific DKO of Rac1 and Rac3 cerebellum (Nakamura et al., 2017), but it was significantly larger in the Cdc42/Rac1-DKO cerebellum than in the control cerebellum (Fig. 5B). This result could explain the mechanism underlying the significant, yet seemingly small difference in the sizes of the control and Cdc42/Rac1-DKO cerebella.

Aberrant positioning of BG and disturbed alignment of radial fibers of BG

To examine the mechanisms underlying CGN retention in the lower half of the ML in Cdc42-KO and Cdc42/Rac1-DKO mice, we focused on radial fibers of BG, which originate

from the somas of BG located in the PCL and terminate at the pial surface of the cerebellum (Yamada and Watanabe, 2002). We prepared 60-μm-thick sections of the cerebellum to obtain 3D information regarding the radial fibers of BG. We immunostained these sections with anti-GFAP and anti-Cre Abs. In addition to the aberrant localization of Cre-positive BG around the PCL in Rac1-KO, Cdc42-KO, and Cdc42/Rac1-DKO mice, obliquely aligned radial fibers of BG were observed in Rac1-KO, Cdc42-KO, and Cdc42/Rac1-DKO mice (Fig. 5A). In Cdc42/Rac1-DKO mice, the obliquely aligned radial fibers were more apparent and thicker than that in the control, Rac1-KO, and Cdc42-KO mice. Concentrated GFAP immunoreactivity in the PCL was obscure in Rac1-KO and Cdc42-KO mice compared with the control, and was almost completely disappeared in Cdc42/Rac1-DKO mice (Fig. 6A). The longitudinal width of the area demonstrating Cre-positive cells around the PCL was significantly different among the control, Rac1-KO, Cdc42-KO, and Cdc42/Rac1-DKO mice; however, the measured number of Cre-positive cells in this area was not (Fig. 6B). In addition, GFAP immunoreactivity at the pial surface of the cerebellum was weak in Cdc42/Rac1-DKO mice when compared to control mice (Fig. 6C).

Functions of the GFAP promoter in BG

Finally, we excluded the possibility that the retained CGNs in the lower half of the ML and aberrantly aligned PCs around the PCL are Cre-positive. Double-immunostaining for Cre and brain lipid-binding protein (BLBP), which is a marker of astrocytes, showed that Cre-positive cells are BLBP-positive in Cdc42/Rac1-DKO mice (16 weeks of age), indicating that the small cells retained in the lower half of the ML are aberrantly localized BG or normal intrinsic astrocytes (Fig. 7A and B). At P10, X-gal staining of cerebella from GFAP-Cre mice indicated that X-gal-positive cells are accumulated in the PCL and cerebellar medulla, where intrinsic astrocytes are abundant (Belvindrah et al., 2006) (Fig. 7C). Cerebellar sections from adult *GFAP-Cre;tdTomato* mice, in which cells with a functioning GFAP promoter exhibit tdTomato (red) fluorescence, showed such fluorescence in small cells adjacent to PCs (Fig. 7D).

These results, along with those presented in Figures 1C and 1D, are consistent with a report indicating that CGNs and PCs do not have GFAP promoter activity (Komine et al., 2007). Our observations suggest that the retained CGNs in the ML and the aberrantly aligned PCs in Cdc42-KO and Cdc42/Rac1-DKO mice are the result of Cdc42 and Rac1 KO in BG.

DISCUSSION

BG are derived from RG after the completion of PC genesis (Buffo and Rossi, 2013), and outwardly migrate to the predicted PCL from E15 to P7 (Yamada and Watanabe, 2002). Concomitant with proliferation, BG condense beneath the multicellular layer of PCs by E18 and are further compacted to form an epithelium-like lining in the PCL by P7 (Yamada and Watanabe, 2002). Komine et al. reported that the activity of the GFAP promoter, which has the same origin as the *GFAP-Cre* TG mouse used in this study, is present starting at E16.5 in BG and is absent in CGNs and PCs (Komine et al., 2007). The above report is consistent with our results, which indicate that GFAP promoter activity is absent in CGNs and PCs (Figs. 1C, 1D, 7A, and 7C). Taken together, the above observations suggest that the aberrant alignment of BG in Rac1-KO, Cdc42-KO, and Cdc42/Rac1-DKO mice is due to impaired compaction of BG in the PCL in the final stage of development (E18-P7).

Here we report a marked exacerbation of cerebellar Cdc42-KO phenotypes after the additional KO of Rac1, in spite of very mild alterations in the cerebellar phenotype (only disturbed alignment of BG) in Rac1-KO mice. Although a Cdc42-mediated Rac activation mechanism that induces a complex of Cdc42–PAR6–aPKC–PAR3–Tiam1–Rac has been reported (Nishimura et al., 2005), we found that the amount of active Rac1 was larger in $MDCK^{Cdc42\text{-}KD}$ cells than $MDCK^{cont}$ cells. This suggests that activation of Rac1 is facilitated by Cdc42 deletion/depletion. These results also suggest that Cdc42 and Rac1 synergistically function in BG during cerebellar corticogenesis, and that some degree of the Cdc42-KO phenotype was compensated for by the upregulation of active Rac1. The mechanism underlying this upregulation of active Rac1 by Cdc42 deletion/depletion should be elucidated by future studies.

BG is reported to be the major cause of impaired radial migration of CGNs (Sidman and Rakic, 1973). Aberrant positioning and maturation of CGNs and PCs induced by impaired polarization of BG, which includes disrupted anchorage of endfeet to the pial basement membrane (BM) of the cerebellar surface, have been also reported. The pial BM is a network of extracellular matrix (ECM) proteins secreted by meningeal fibroblasts (Sievers et al.,

1994). B_1-integrin and α-dystroglycan (αDG) are receptors for laminin, which is a component of the ECM. Mouse lines lacking β_1-integrin–integrin-linked kinase (ILK) signaling (involving the Abl non-receptor family tyrosine kinases) (Belvindrah et al., 2006; Qiu et al., 2010) or αDG–dystrophin signaling (involving the O-Glycosylation enzymes of αDG) (Satz et al., 2008) have aberrant localization of BG and PCs associated with disrupted anchoring of BG endfeet to the pial surface of the cerebellum. In addition, Belvindrah et al. reported that the amount of GTP-bound Cdc42 is drastically reduced at the tips of outgrowing BG radial fibers in *ILK*-KO mice (Belvindrah et al., 2006), and that Rac1 is not involved in this reduction (Belvindrah et al., 2006; Qiu et al., 2010). KO of *Ric-8a*, which is a non-receptor guanine nucleotide exchange factor that regulates Gα subunits, also leads to aberrant localization of BG and PCs and impaired radial migration of CGNs because of the disrupted anchoring of BG endfeet to the pial surface (Ma et al., 2012). Furthermore, the above studies pointed out that deletion of these molecules from BG, but not CGNs, is critical for the observed phenotypes (Frick et al., 2012; Ma et al., 2012; Qiu et al., 2010). Thus, the phenotypes observed in our Cdc42/Rac1-DKO mice and in the abovementioned KO mouse lines are probably due to the same mechanism, by which the establishment or maintenance of the endfeet of BG radial fibers is impaired to varying degrees (mildly impaired in the case of Cdc42/Rac1-DKO mice).

While there is disturbed alignment of PCs in Cdc42-KO and Cdc42/Rac1-DKO mice, neither Cdc42 nor Rac1 are deleted in PCs. Deletion of *Notch1*, *Notch2*, a downstream target of Notch (*Recombination Signal Binding Protein For Immunoglobulin Kappa J Region* (*RBPJ*)) (Komine et al., 2007), or a ligand of Notch (*Delta-like1*) (Hiraoka et al., 2013) in BG leads to irregularities in BG positioning and disorganized BG radial fibers, but not disturbed alignment of PCs, as the above molecules are responsible for BG-BG interactions. Deletion of *density-regulated protein* (*DENR*), which is a neuron-specific Notch ligand in PCs and is tightly associated with BG radial fibers expressing Notch, led to reduced numbers of BG radial fibers and aberrant localization of BG, but not a disturbed alignment of PCs (Eiraku et al., 2005). The differences between the KO mouse lines containing abnormal BG and normal

PC positioning, and those lines (i.e., those mentioned in the adjacent paragraph, including the Cdc42/Rac1-DKO mice) with both abnormal BG and disturbed PC positioning, may be due to differences in the severity of abnormality in the BG radial fibers.

In addition to the abovementioned KO-mice lines, *phosphatase and tensin homolog* (*PTEN*) KO in mice under the control of the GFAP promoter shows leads to numerous branched and thickened BG radial fibers with abnormal anchorage to the pial surface of the cerebellum. This leads to the accumulation of CGNs in the ML and the aberrant localization of PCs (Yue et al., 2005). Cdc42 has been reported to be involved in epithelial polarization via PTEN-mediated apical segregation of phosphoinositides (Martin-Belmonte et al., 2007). This further supports the involvement of Cdc42 in the differentiation and function of BG. Moreover, DKO of *Abr* and *Bcr*, which are GTPase-activating proteins (GAPs) of Cdc42 and Rac, leads to prematurely terminated and disorganized endfeet of BG radial fibers, aberrant localization of BG, and ectopic CGNs in and on the surface of the ML, although it has no effect on the alignment of PCs (Kaartinen et al., 2001). Thus, appropriate regulation of Cdc42 and Rac activities in BG may also be required for proper morphology and function of BG.

Growth factor signaling involving receptor tyrosine kinases such as ErbB and FGFR is important in several ways for the differentiation and maturation of BG, as well as the interaction of BG and CGNs (Buffo and Rossi, 2013). Stimulation of ErbB2 and ErbB4 by neuregulin 1 was reported to be important for the morphological establishment of RG (Schmid et al., 2003), and for the contact between BG and CGNs allowing for the radial migration of CGNs (Rio et al., 1997). In addition, mice with a DKO of *FGFR1* and *FGFR2* under the *GFAP* promoter reportedly have fewer BG, and abnormal morphology of both the remaining BG and the cerebellum (Muller Smith et al., 2012). Because DNA microarray analysis revealed that the predominant subtypes in WT primary astrocytes are *ErbB1* (also referred to as EGFR) and *ErbB2* of the *ErbB1–4* family, and *FGFR1* and *FGFR3* of the *FGFR1–4* family (Table S1, GES106141), we focused on ErbB1, ErbB2, FGFR1, and FGFR3. None of their mRNA or protein levels were significantly changed in CDC42/RAC1-DKD U87 cells versus the controls upon DNA microarray analysis (Table S2,

GES106142; Fig. S2B) and immunoblotting (Fig. S2C). In addition to ErbB1 and ErbB2, we analyzed ErbB4, and then chose to include ErbB3 as it is also reported to be involved in the proliferation and development of BG and the subsequent radial migration of CGNs (Sathyamurthy et al., 2015). Although mRNA levels of *ErbB4* in control U87 cells (12.0 in signal intensity units) were quite low compared with those of *ErbB2* (290~360 units), they increased about 8-fold in CDC42/RAC1-DKD U87 cells (95.9 units, Table S2). In contrast, *ErbB3* mRNA was not significantly changed by DKD of *CDC42/RAC1* (from 224.8 to 271.4 units, Table S2). Although neuregulin 1 on CGNs can bind to ErbB4 expressed on BG (Rio et al., 1997), *neuregulin 1* mRNA was significantly downregulated in CDC42/RAC1-DKD U87 cells (from 5281.1 to 2217.3 units, Table S2), and was quite high in WT primary astrocytes (12123.7 units, nearly half the signal level of *Rac1*, Table S1). These data suggest that the inverse signaling pathway may be present, with BG-expressed neuregulin 1 binding to CGN-expressed ErbB. Moreover, CDC42/RAC1-DKD U87 cells demonstrated upregulated *neuregulin 3* (from 13.8 to 88.7 units) and *Notch3* (from 5726.0 to 11487.2 units) mRNAs (Table S2). Upregulation of *ErbB4*, *neuregulin 3*, and *Notch3* in CDC42/RAC1-DKD U87 cells may be the result of a compensation mechanism for the impaired BG morphology and radial migration of CGNs in the Rac1/Cdc42-DKO cerebellum. Because the expression and function of ErbB4 in BG have been well-studied (Rio et al., 1997), we focused on studying the expression of neuregulin 1 and Notch3 in BG during cerebellar development (at P10). As expected by the high levels of expression of neuregulin 1 and Notch3 mRNAs in WT primary astrocytes (12123.7 and 5012.0 units, respectively, Table S1), both neuregulin 1 and Notch3 were detected in BG by immunostaining. Neuregulin 1 was more easily detected (i.e., was denser) than Notch3 in BG (Fig. S3). Previous studies have demonstrated both the comparable expression levels of neuregulin 1 in BG and PCs (Law et al., 2004) and the expression of Notch3 in BG (de Oliveira-Carlos et al., 2013; Irvin et al., 2001) that were seen in these experiments. In the present study, we were unable to determine the exact molecular mechanism producing impaired radial migration of CGNs in the Rac1/Cdc42-DKO mice (*GFAP-Cre;Cdc42* $^{flox/flox}$). Further studies are required to clarify and verify whether the

mechanism is neuregulin 1- or Notch3-mediated.

Gliophilic and neurophilic migration have been reported to be required for the radial migration of CGNs (Rakic, 1990). Radial migration of CGNs along BG radial fibers is classified as gliophilic migration. Contact between BG radial fibers and descending CGNs has been reported in studies using electron microscopes (Rakic, 1971; Yamada and Watanabe, 2002). We recently reported that mice with deletion of Rac (Rac1 and Rac3) in CGNs (using the *Atoh1-Cre* TG mouse) have severe ataxia owing to agenesis of the IGL. Rac-KO CGNs at the deep layer of the EGL undergo apoptosis at around P8 owing to defects in the final differentiation of their dendrites, which are essential for neurophilic migration (Nakamura et al., 2017). Here we report that there is normal radial migration of CGNs in mice with deletion of Rac in BG (*GFAP-Cre;Rac1*$^{flox/flox}$) and impaired radial migration of CGNs in the lower half of the ML in mice with deletion of Cdc42 in BG (*GFAP-Cre;Cdc42* $^{flox/flox}$). We also found that the phenotypes observed following single deletion of Cdc42 were exacerbated by the additional deletion of Rac. These results indicate that 1) gliophilic migration involving Cdc42 and Rac plays important roles during the late phase of CGN radial migration, 2) neurophilic migration involving Rac plays essential roles during the early phase of CGN radial migration.

In summary, radial migration of CGNs is regulated by synchronizing the regulation of Cdc42 and Rac in BG (gliophilic migration) and Rac in CGN (neurophilic migration). Gliophilic migration involving Cdc42 and Rac plays important roles during the late phase and neurophilic migration involving Rac is essential during the early phase (Fig. 8).

Acknowledgements

We thank Prof. Atsu Aiba (The University of Tokyo) for providing the *Cdc42*^{flox} and *Rac1*^{flox} mice. We are also thankful to Prof. David H. Gutmann (Washington University) for providing the *GFAP-Cre* transgenic mice. This work was supported by the Japan Society for the Promotion of Science (JSPS) KAKENHI Grants 17H04042 (to TU) and 17H04032 (to NS), and by Grants-in Aid for the Cooperative Research Project from the Institute of Natural Medicine, University of Toyama in 2015 and 2016 (to TU).

Conflict of interest

The authors declare that they have no conflicts of interest regarding the contents of this article.

Author contributions

TU and NS planned the project. IS, TU, MH, HM, TN, MS, and CT performed the histological experiments. TU, MH, and HM performed the molecular and cellular biology experiments. HK performed the experiments necessary to provide genetically engineered mice. IS, TU, and NS analyzed the data, and TU wrote the manuscript.

REFERENCES

Bajenaru, M.L., Zhu, Y., Hedrick, N.M., Donahoe, J., Parada, L.F., Gutmann, D.H., 2002. Astrocyte-specific inactivation of the neurofibromatosis 1 gene (NF1) is insufficient for astrocytoma formation. Mol Cell Biol 22, 5100-5113.

Belvindrah, R., Nalbant, P., Ding, S., Wu, C., Bokoch, G.M., Muller, U., 2006. Integrin-linked kinase regulates Bergmann glial differentiation during cerebellar development. Mol Cell Neurosci 33, 109-125.

Borrell, V., Gotz, M., 2014. Role of radial glial cells in cerebral cortex folding. Curr Opin Neurobiol 27, 39-46.

Bosco, E.E., Mulloy, J.C., Zheng, Y., 2009. Rac1 GTPase: a "Rac" of all trades. Cell Mol Life Sci 66, 370-374.

Buffo, A., Rossi, F., 2013. Origin, lineage and function of cerebellar glia. Prog Neurobiol 109, 42-63.

Chedotal, A., 2010. Should I stay or should I go? Becoming a granule cell. Trends Neurosci 33, 163-172.

de Oliveira-Carlos, V., Ganz, J., Hans, S., Kaslin, J., Brand, M., 2013. Notch receptor expression in neurogenic regions of the adult zebrafish brain. PLoS One 8, e73384.

Eiraku, M., Tohgo, A., Ono, K., Kaneko, M., Fujishima, K., Hirano, T., Kengaku, M., 2005. DNER acts as a neuron-specific Notch ligand during Bergmann glial development. Nat Neurosci 8, 873-880.

Frick, A., Grammel, D., Schmidt, F., Poschl, J., Priller, M., Pagella, P., von Bueren, A.O., Peraud, A., Tonn, J.C., Herms, J., Rutkowski, S., Kretzschmar, H.A., Schuller, U., 2012. Proper cerebellar development requires expression of beta1-integrin in Bergmann glia, but not in granule neurons. Glia 60, 820-832.

Hatten, M.E., Alder, J., Zimmerman, K., Heintz, N., 1997. Genes involved in cerebellar cell specification and differentiation. Curr Opin Neurobiol 7, 40-47.

Heasman, S.J., Ridley, A.J., 2008. Mammalian Rho GTPases: new insights into their functions from in vivo studies. Nat Rev Mol Cell Biol 9, 690-701.

Hiraoka, Y., Komine, O., Nagaoka, M., Bai, N., Hozumi, K., Tanaka, K., 2013. Delta-like 1 regulates Bergmann glial monolayer formation during cerebellar development. Mol Brain 6, 25.

Irvin, D.K., Zurcher, S.D., Nguyen, T., Weinmaster, G., Kornblum, H.I., 2001. Expression patterns of Notch1, Notch2, and Notch3 suggest multiple functional roles for the Notch-DSL signaling system during brain development. J Comp Neurol 436, 167-181.

Ishii, T., Ueyama, T., Shigyo, M., Kohta, M., Kondoh, T., Kuboyama, T., Uebi, T., Hamada, T., Gutmann, D.H., Aiba, A., Kohmura, E., Tohda, C., Saito, N., 2016. A Novel Rac1-GSPT1 Signaling Pathway Controls Astrogliosis Following Central Nervous System Injury. J Biol Chem 292, 1240-1250.

Kaartinen, V., Gonzalez-Gomez, I., Voncken, J.W., Haataja, L., Faure, E., Nagy, A., Groffen, J., Heisterkamp, N., 2001. Abnormal function of astroglia lacking Abr and Bcr RacGAPs. Development 128, 4217-4227.

Komine, O., Nagaoka, M., Watase, K., Gutmann, D.H., Tanigaki, K., Honjo, T., Radtke, F., Saito, T., Chiba, S., Tanaka, K., 2007. The monolayer formation of Bergmann glial cells is regulated by Notch/RBP-J signaling. Dev Biol 311, 238-250.

Komuro, H., Yacubova, E., Rakic, P., 2001. Mode and tempo of tangential cell migration in the cerebellar external granular layer. J Neurosci 21, 527-540.

Law, A.J., Shannon Weickert, C., Hyde, T.M., Kleinman, J.E., Harrison, P.J., 2004. Neuregulin-1 (NRG-1) mRNA and protein in the adult human brain. Neuroscience 127, 125-136.

Ma, S., Kwon, H.J., Huang, Z., 2012. Ric-8a, a guanine nucleotide exchange factor for heterotrimeric G proteins, regulates bergmann glia-basement membrane adhesion during cerebellar foliation. J Neurosci 32, 14979-14993.

Martin-Belmonte, F., Gassama, A., Datta, A., Yu, W., Rescher, U., Gerke, V., Mostov, K., 2007. PTEN-mediated apical segregation of phosphoinositides controls epithelial morphogenesis through Cdc42. Cell 128, 383-397.

Muller Smith, K., Williamson, T.L., Schwartz, M.L., Vaccarino, F.M., 2012. Impaired motor coordination and disrupted cerebellar architecture in Fgfr1 and Fgfr2 double knockout mice. Brain Res 1460, 12-24.

Nakamura, T., Ueyama, T., Ninoyu, Y., Sakaguchi, H., Choijookhuu, N., Hishikawa, Y., Kiyonari, H., Kohta, M., Sakahara, M., de Curtis, I., Kohmura, E., Hisa, Y., Aiba, A., Saito, N., 2017. Novel role of Rac-Mid1 signaling in medial cerebellar development. Development 144, 1863-1875.

Nishimura, T., Yamaguchi, T., Kato, K., Yoshizawa, M., Nabeshima, Y., Ohno, S., Hoshino, M., Kaibuchi, K., 2005. PAR-6-PAR-3 mediates Cdc42-induced Rac activation through the Rac GEFs STEF/Tiam1. Nat Cell Biol 7, 270-277.

Pekny, M., Pekna, M., Messing, A., Steinhauser, C., Lee, J.M., Parpura, V., Hol, E.M., Sofroniew, M.V., Verkhratsky, A., 2016. Astrocytes: a central element in neurological diseases. Acta Neuropathol 131, 323-345.

Qin, Y., Meisen, W.H., Hao, Y., Macara, I.G., 2010. Tuba, a Cdc42 GEF, is required for polarized spindle orientation during epithelial cyst formation. J Cell Biol 189, 661-669.

Qiu, Z., Cang, Y., Goff, S.P., 2010. Abl family tyrosine kinases are essential for basement membrane integrity and cortical lamination in the cerebellum. J Neurosci 30, 14430-14439.

Rakic, P., 1971. Neuron-glia relationship during granule cell migration in developing cerebellar cortex. A Golgi and electronmicroscopic study in Macacus Rhesus. J Comp Neurol 141, 283-312.

Rakic, P., 1990. Principles of neural cell migration. Experientia 46, 882-891.

Rio, C., Rieff, H.I., Qi, P., Khurana, T.S., Corfas, G., 1997. Neuregulin and erbB receptors play a critical role in neuronal migration. Neuron 19, 39-50.
Sathyamurthy, A., Yin, D.M., Barik, A., Shen, C., Bean, J.C., Figueiredo, D., She, J.X., Xiong, W.C., Mei, L., 2015. ERBB3-mediated regulation of Bergmann glia proliferation in cerebellar lamination. Development 142, 522-532.
Satz, J.S., Barresi, R., Durbeej, M., Willer, T., Turner, A., Moore, S.A., Campbell, K.P., 2008. Brain and eye malformations resembling Walker-Warburg syndrome are recapitulated in mice by dystroglycan deletion in the epiblast. J Neurosci 28, 10567-10575.
Schmid, R.S., McGrath, B., Berechid, B.E., Boyles, B., Marchionni, M., Sestan, N., Anton, E.S., 2003. Neuregulin 1-erbB2 signaling is required for the establishment of radial glia and their transformation into astrocytes in cerebral cortex. Proc Natl Acad Sci U S A 100, 4251-4256.
Sidman, R.L., Rakic, P., 1973. Neuronal migration, with special reference to developing human brain: a review. Brain Res 62, 1-35.
Sievers, J., Pehlemann, F.W., Gude, S., Berry, M., 1994. Meningeal cells organize the superficial glia limitans of the cerebellum and produce components of both the interstitial matrix and the basement membrane. J Neurocytol 23, 135-149.
Takano, T., Xu, C., Funahashi, Y., Namba, T., Kaibuchi, K., 2015. Neuronal polarization. Development 142, 2088-2093.
Ueyama, T., Geiszt, M., Leto, T.L., 2006. Involvement of Rac1 in activation of multicomponent Nox1- and Nox3-based NADPH oxidases. Molecular and cellular biology 26, 2160-2174.
Ueyama, T., Ninoyu, Y., Nishio, S.Y., Miyoshi, T., Torii, H., Nishimura, K., Sugahara, K., Sakata, H., Thumkeo, D., Sakaguchi, H., Watanabe, N., Usami, S.I., Saito, N., Kitajiri, S.I., 2016. Constitutive activation of DIA1 (DIAPH1) via C-terminal truncation causes human sensorineural hearing loss. EMBO Mol Med 8, 1310-1324.
Ueyama, T., Sakaguchi, H., Nakamura, T., Goto, A., Morioka, S., Shimizu, A., Nakao, K., Hishikawa, Y., Ninoyu, Y., Kassai, H., Suetsugu, S., Koji, T., Fritzsch, B., Yonemura, S., Hisa, Y., Matsuda, M., Aiba, A., Saito, N., 2014. Maintenance of stereocilia and apical junctional complexes by Cdc42 in cochlear hair cells. J Cell Sci 127, 2040-2052.
Ueyama, T., Tatsuno, T., Kawasaki, T., Tsujibe, S., Shirai, Y., Sumimoto, H., Leto, T.L., Saito, N., 2007. A regulated adaptor function of $p40^{phox}$: distinct $p67^{phox}$ membrane targeting by $p40^{phox}$ and by $p47^{phox}$. Mol Biol Cell 18, 441-454.
Xu, H., Yang, Y., Tang, X., Zhao, M., Liang, F., Xu, P., Hou, B., Xing, Y., Bao, X., Fan, X., 2013. Bergmann glia function in granule cell migration during cerebellum development. Mol Neurobiol 47, 833-844.
Yamada, K., Watanabe, M., 2002. Cytodifferentiation of Bergmann glia and its relationship with Purkinje cells. Anat Sci Int 77, 94-108.

Yuasa, S., Kawamura, K., Ono, K., Yamakuni, T., Takahashi, Y., 1991. Development and migration of Purkinje cells in the mouse cerebellar primordium. Anat Embryol (Berl) 184, 195-212.
Yue, Q., Groszer, M., Gil, J.S., Berk, A.J., Messing, A., Wu, H., Liu, X., 2005. PTEN deletion in Bergmann glia leads to premature differentiation and affects laminar organization. Development 132, 3281-3291.

FIGURE LEGENDS

Figure 1: Generation of Rac1- and Cdc42-KO mice using *GFAP-Cre* mice

A. RT-PCR was performed using cDNA obtained from WT primary astrocytes and specific primer-pairs of *Rac1*, *Rac3*, and *Cdc42*. The predicted sizes of the amplified *Rac1*, *Rac3*, and *Cdc42* bands are 454, 440, and 579 base pairs (bp). NC: negative control (without cDNA). n= 3.

B. Illustration of the genetic construction of *GFAP-Cre* mice. The LacZ gene with a nuclear localization signal (NLS) is located under the internal ribosome entry site (IRES) sequence.

C. Brains from 24-week-old control and *GFAP-Cre* mice were fixed. Sections of the cerebral cortex (left) and cerebellar cortex (right) were subjected to X-gal staining and GFAP immunostaining. Scale bars: 100 μm. n= 3.

D. Brains from 13-week-old *GFAP-Cre* mice were fixed. Sections from the cerebellar cortex were subjected to immunostaining for GFAP (green) and Cre (red) (left) or calbindin (green) and Cre (red) (right). GFAP-positive radial fibers of Bergmann glia originate from cells with Cre-positive nuclei (left). The Cre-positive cells are located between Purkinje cells (asterisks) (right). Scale bars: 50 μm. n≥ 5.

E, Primary astrocytes obtained from control and *GFAP-Cre;Rac1*$^{flox/flox}$ (Rac1-KO) and *GFAP-Cre;Cdc42*$^{flox/flox}$ (Cdc42-KO) mice were subjected to immunoblotting using Rac1 and Cdc42 antibodies, respectively. Comparable loading of proteins was confirmed using a tubulin-α antibody. n= 2.

Figure 2: Impaired development of the cerebellar cortex in Cdc42-KO and Cdc42/Rac1-DKO mice

Sections of cerebral cortex (A), cerebellar cortex (B), and cerebellum (C) from adult control, *GFAP-Cre;Rac1*$^{flox/flox}$ (Rac1-KO), *GFAP-Cre;Cdc42*$^{flox/flox}$ (Cdc42-KO), and *GFAP-Cre;Cdc42*$^{flox/flox}$*;Rac1*$^{flox/flox}$ (Cdc42/Rac1-DKO) mice were subjected to Nissl staining. Scale bars: 100 μm (A, B), 1 mm (C).

A. No apparent abnormalities are observed in the cerebral cortex of control, Rac1-KO, Cdc42-KO, or Cdc42/Rac1-DKO mice. n= 3.

B. Densely stained small cells accumulate in the lower half of the molecular layer (lines) in Cdc42-KO and Cdc42/Rac1-DKO mice. Lightly stained large cells are aligned in multiple layers (bidirectional arrows) in Cdc42-KO and Cdc42/Rac1-DKO mice. The number of densely stained small cells was quantified (n= 3, * $P<0.05$, ** $P<0.01$, and **** $P<0.0001$ by Bonferroni's *post hoc* test following one-way ANOVA).

C. Low magnification images of control, Cdc42-KO, and Cdc42/Rac1-DKO cerebellum. Abnormal corticogenesis (arrowheads) is observed throughout the cerebella of Cdc42-KO and Cdc42/Rac1-DKO (more severe) mice. The longest length of the cerebellum was measured and expressed as a percentage of the control (n=4, * $P<0.05$ and ** $P<0.01$ by Bonferroni's *post hoc* test following one-way ANOVA). Rectangles indicate the regions from which nearly all images in the present study were obtained.

Figure 3: Aberrant positioning of BG and PCs

Sections of cerebellar cortex from 16-week-old control, *GFAP-Cre;Rac1*$^{flox/flox}$ (Rac1-KO), *GFAP-Cre;Cdc42*$^{flox/flox}$ (Cdc42-KO), and *GFAP-Cre;Cdc42*$^{flox/flox}$*;Rac1*$^{flox/flox}$ (Cdc42/Rac1-DKO) mice were subjected to immunostaining for NeuN (A), Cre (B), PKCγ (C), and GFAP (D). Scale bars: 100 μm.

A. Cerebellar granule neurons (CGNs) were stained using a NeuN antibody. Lines indicate accumulation of CGNs in the lower half of the molecular layer (ML). The number of NeuN-positive cells in the ML was quantified (n= 3, ** $P<0.01$, *** $P<0.001$, and **** $P<0.0001$ by Bonferroni's *post hoc* test following one-way ANOVA).

B. Bergmann glia (BG) were stained using a Cre antibody. Bidirectional arrows indicate aberrantly aligned BG around the Purkinje cell layer (PCL). The number of Cre-positive cells around the PCL was also quantified (n=8, no statistically significant differences).

C. Purkinje cells (PCs) were stained using a PKCγ antibody. Arrowheads indicate aberrantly aligned PCs. The number of PKCγ-positive cells was also quantified (n=8, no statistically

significant differences).

D. Radial fibers of BG were stained using a GFAP antibody. No clear border between the ML and the internal granule layer (arrows) is observed in Cdc42/Rac1-DKO mice. n=5

Figure 4: Impaired radial migration of CGNs in Cdc42-KO and Cdc42/Rac1-DKO mice during cerebellar corticogenesis

Sections of cerebellar cortex from 3- to 21-day-old (P3 to P21) mice (control, *GFAP-Cre;Cdc42*$^{flox/flox}$ [Cdc42-KO], and *GFAP-Cre;Cdc42*$^{flox/flox}$*;Rac1*$^{flox/flox}$ [Cdc42/Rac1-DKO]) were subjected to Nissl staining. Bidirectional arrows in images from P5 to P21 Cdc42-KO and Cdc42/Rac1-DKO mice indicate accumulated densely stained small cerebellar granule neurons (CGNs) in the lower half of the molecular layer. Lightly stained Purkinje cells (arrowheads) aligned in multiple layers are apparent in Cdc42/Rac1-DKO mice. Asterisks: external granule layer. The number of densely stained small cells in the ML at P21 was quantified (n= 3, ** P<0.01 and **** P<0.0001 by Bonferroni's *post hoc* test following one-way ANOVA). Scale bars: 100 μm.

Figure 5: Normal proliferation of BG and detection of apoptosis in the Cdc42/Rac1-DKO cerebellum

A. EdU was injected into control and *GFAP-Cre;Cdc42*$^{flox/flox}$*;Rac1*$^{flox/flox}$ (Cdc42/Rac1-DKO) mice at P3.5, and samples were fixed at 24 h after injection. Sagittal sections of the control and *Cdc42/Rac1*-DKO cerebellum were obtained. EdU labeling of cells around the predicted Purkinje cell layer (PCL, indicated by bidirectional arrows) was quantified (n=4, no statistically significant difference). EGL: external granule layer. ML: molecular layer. Scale bars: 25 μm.

B. Sagittal sections of P4 control and Cdc42/Rac1-DKO cerebellum were subjected to immunostaining for active caspase-3 with methyl green counterstaining. The number of active caspase 3-positive cells (arrowheads) around the predicted PCL (indicated by bidirectional arrows) was then quantified (n= 3, ** P<0.01 by Student's *t*-test). Inset:

Magnified image of the boxed area. Scale bars: 100 μm.

Figure 6: Aberrant positioning of BG and disturbed alignment of BG radial fibers

A. Thick (60 μm) sections of cerebellar cortex from 16-week-old control, *GFAP-Cre;Rac1*$^{flox/flox}$ (Rac1-KO), *GFAP-Cre;Cdc42*$^{flox/flox}$ (Cdc42-KO), and *GFAP-Cre;Cdc42*$^{flox/flox}$*;Rac1*$^{flox/flox}$ (Cdc42/Rac1-DKO) mice were immunostained using GFAP (green) and Cre (red) antibodies. After images (0.5-μm pitch) were obtained using a confocal laser fluorescence microscope, 2D images were reconstructed. Aberrantly aligned Bergmann glia (BG) stained by Cre are observed in Rac1-KO, Cdc42-KO, and Cdc42/Rac1-DKO mice. Arrows indicate oblique and thick radial fibers of BG in Cdc42/Rac1-DKO mice. Note the absence of a clear border between the ML and the internal granule layer in Cdc42/Rac1-DKO mice. Scale bars: 50 μm. n= 5.

B. The longitudinal width (indicated by bidirectional arrows in A) of the area demonstrating Cre-positive cells around the Purkinje cell layer (PCL) (n= 10, ** $P<0.01$, *** $P<0.001$, and **** $P<0.0001$ by Bonferroni's *post hoc* test following one-way ANOVA) and the number of Cre-positive cells in this area (n= 6, no statistically significant difference) were quantified.

C. Normal sections (20 μm) of cerebellar cortex from 16-week-old control and Cdc42/Rac1-DKO mice were immunostained using a GFAP antibody. Arrowheads indicate the weak staining of BG endfeet at the cerebellar surface in Cdc42/Rac1-DKO mice when compared to that in control mice. Scale bars: 50 μm. n= 5.

Figure 7: Cre-positive cells in the ML are BLBP-positive

A and B. Sections of cerebellar cortex from 16-week-old *GFAP-Cre;Cdc42*$^{flox/flox}$*;Rac1*$^{flox/flox}$ (Cdc42/Rac1-DKO) (A) and control (B) mice were subjected to immunostaining using BLBP and Cre antibodies. Arrowheads indicate double-positive cells in the molecular layer (ML). Scale bars: 50 μm. n= 3.

C. A section of cerebellar cortex from a 10-day-old *GFAP-Cre* mouse was subjected to X-gal

staining. Scale bars: 100 μm. n= 3.

D. Laser confocal microscope image of a section of cerebellar cortex from an adult *GFAP-Cre;tdTomato* mouse. Arrowheads indicate tdTomato fluorescence-positive Bergmann glia adjacent to Purkinje cells (asterisks). The rectangular inset represents the magnified image of the region indicated by the rectangle. Scale bars: 50 μm. n=2.

Figure 8: Radial migration of CGNs using both neurophilic and gliophilic migration

A. The illustration shows the neurophilic migration of cerebellar granule neurons (CGNs), which use their own dendrites (arrowhead) for radial migration. Rac (Rac1 and Rac3) is essential for the early phase of radial migration in CGNs (Nakamura et al., 2017).

B. The illustration shows gliophilic migration of CGNs, which require contact with radial fibers of Bergmann glia (BG, arrowheads) during their radial migration. Cdc42 and Rac1, but more so Cdc42, in BG play critical roles during the late phase (in the lower part of the molecular layer (ML)) of radial migration. EGL: external granule cells. PCL: Purkinje cell layer.

Figure 1, Sakamoto et al.

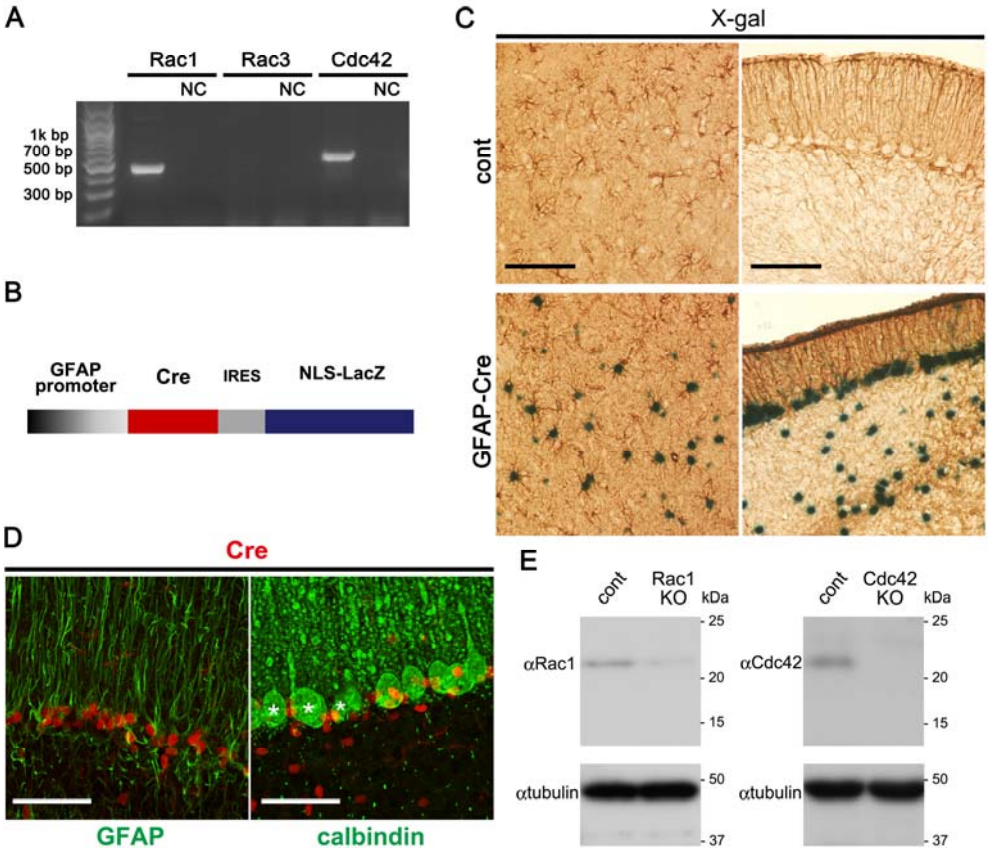

Figure 2, Sakamoto et al.

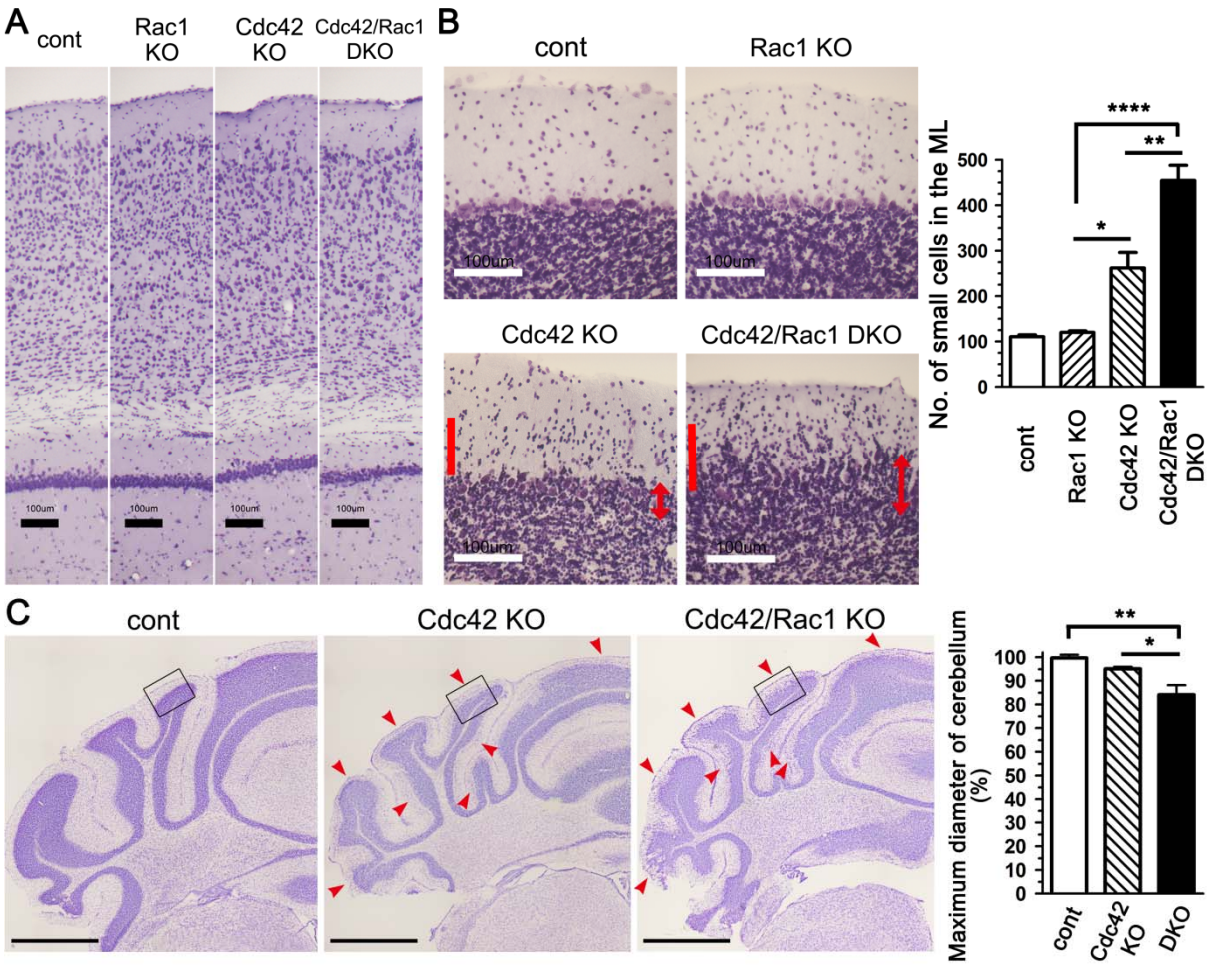

Figure 3, Sakamoto et al.

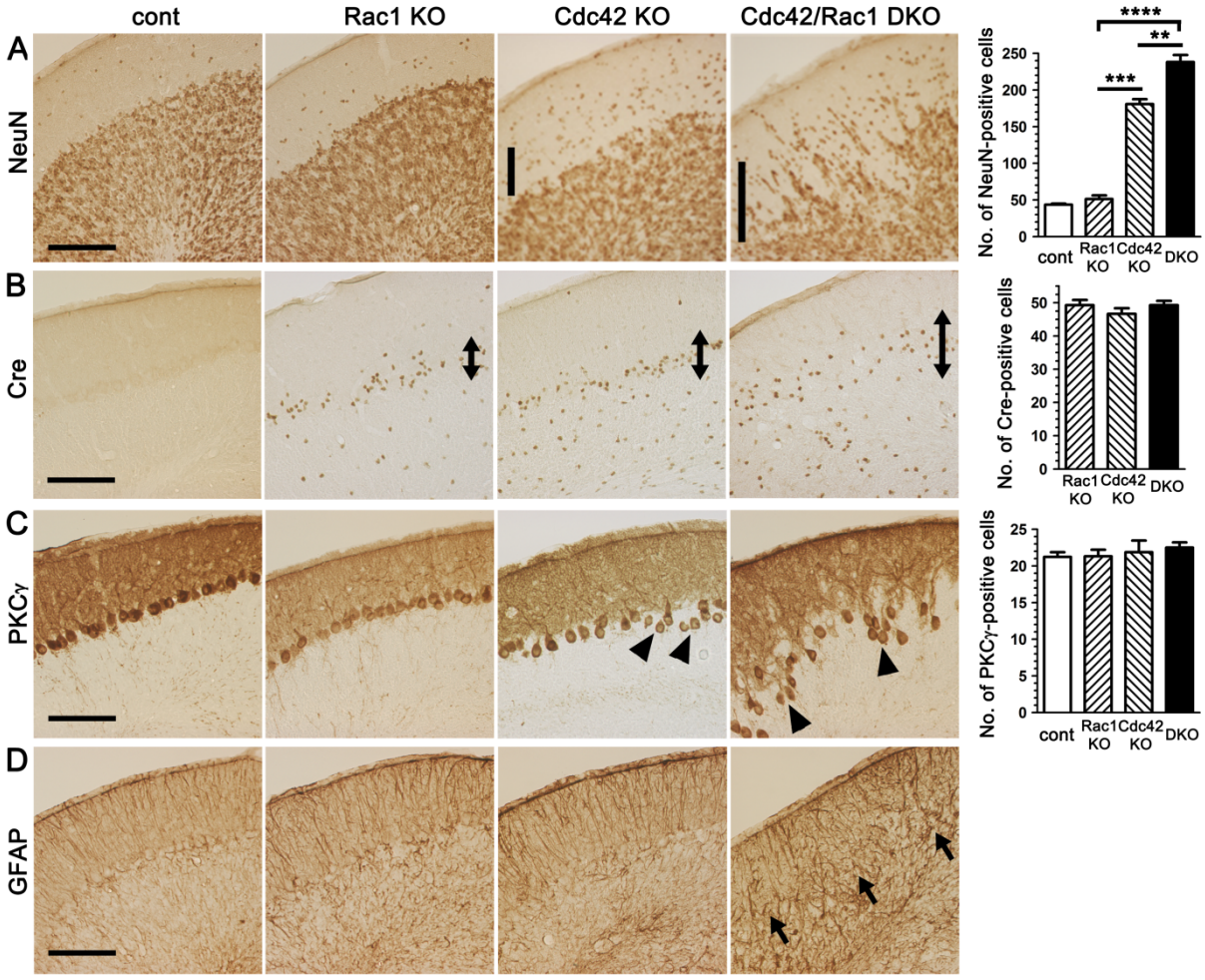

Figure 4, Sakamoto et al.

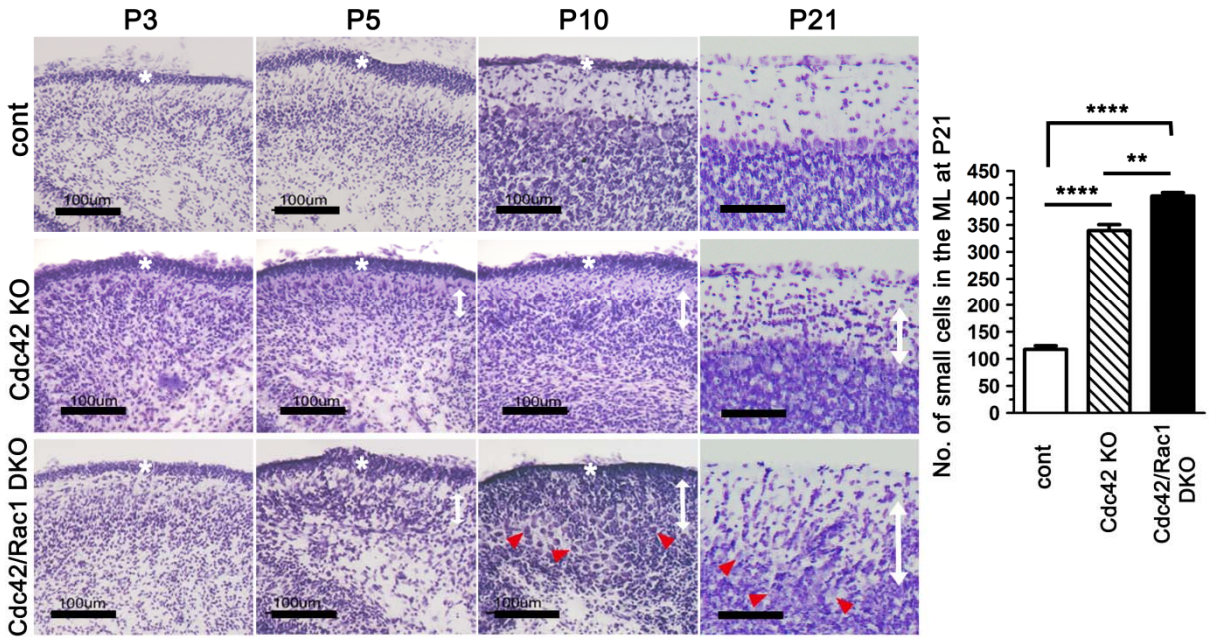

Figure 5, Sakamoto et al.

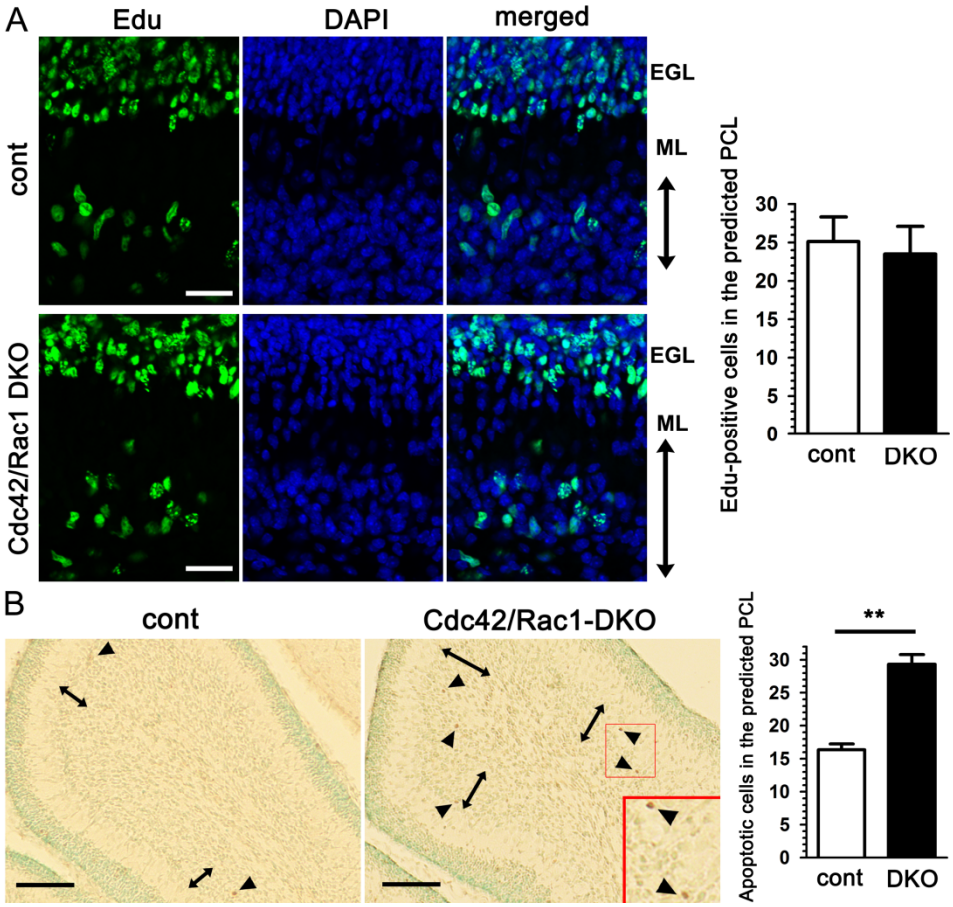

Figure 6, Sakamoto et al.

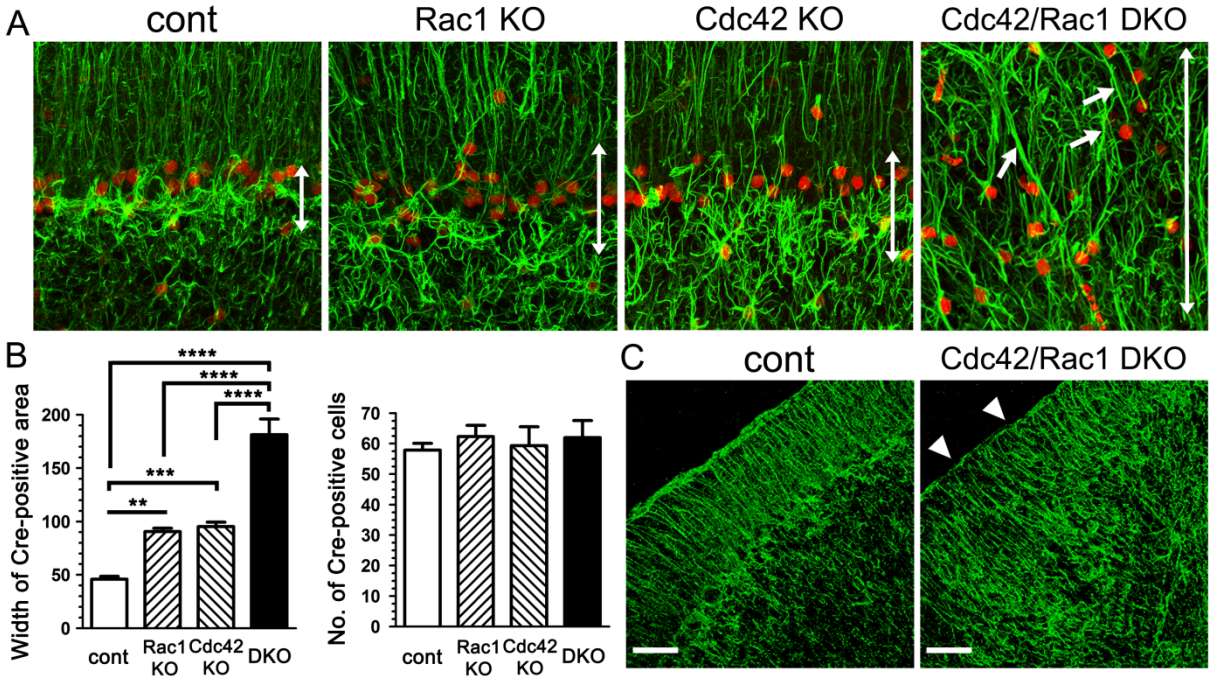

Figure 7, Sakamoto et al.

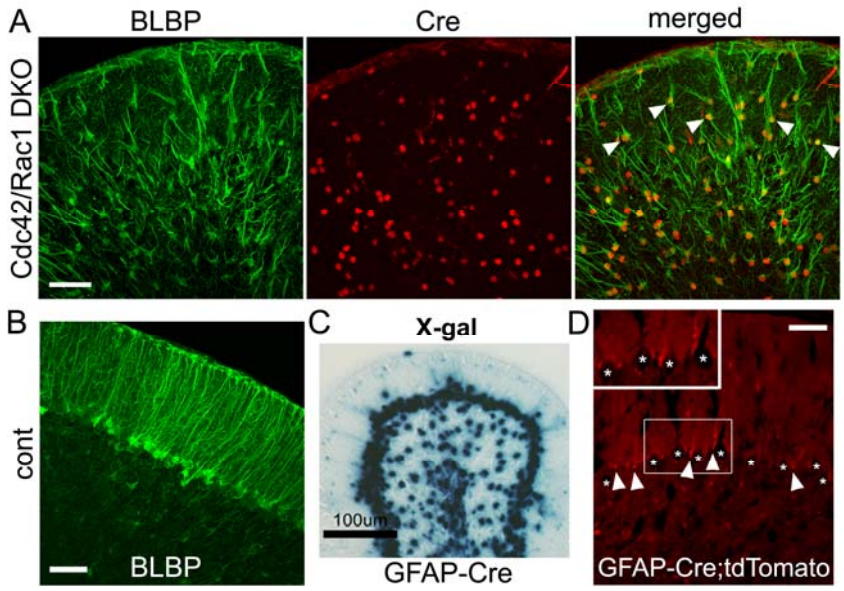

Figure 8, Sakamoto et al.

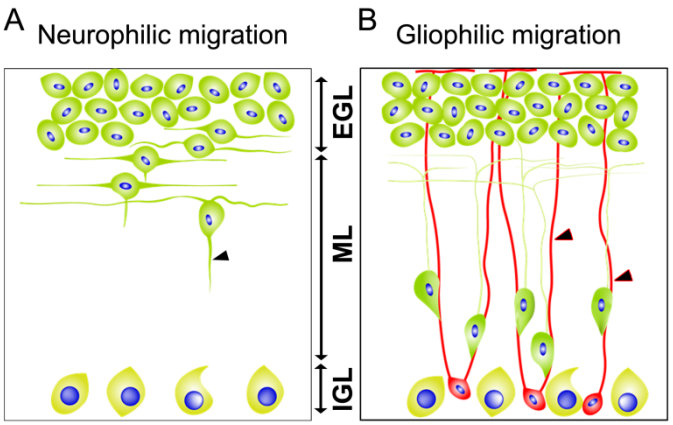

Supplementary Figure 1, Sakamoto et al.

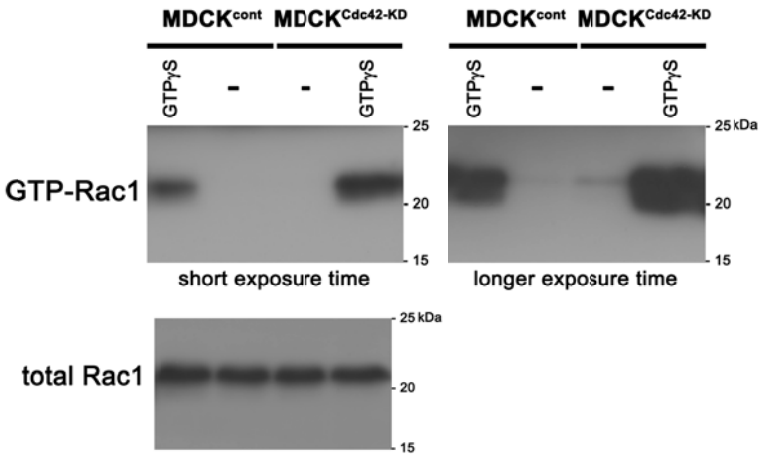

Supplementary Figure 2, Sakamoto et al.

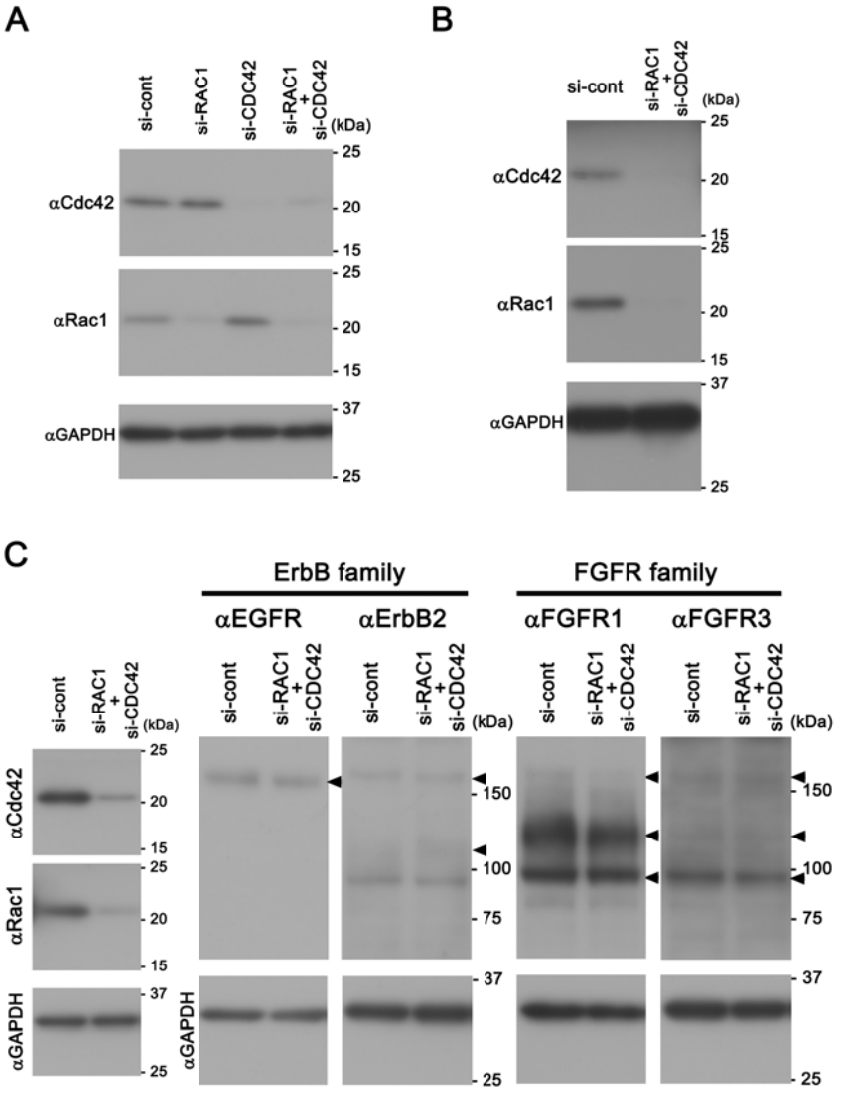

Supplementary Figure 3, Sakamoto et al.